Supramolecular Chemistry

DOI: 10.1002/ange.200601961

Cocrystallization and Encapsulation of a Fluorophore with Hexameric Pyrogallol[4]arene Nanocapsules: Structural and Fluorescence Studies**

Scott J. Dalgarno, Daniel B. Bassil, Sheryl A. Tucker, and Jerry L. Atwood**

The ability to encapsulate space is a concept that has attracted considerable attention in recent years. Significant advances have been made towards the formation of stable noncovalent assemblies that are voluminous and that show potential for molecular encapsulation.[1] We, amongst others, have been interested in the formation of large hydrogen-bonded nanocapsules based on *C*-methylresorcin[4]arene (CMRC, **1**; Figure 1) or the closely related *C*-alkylpyrogallol[4]arenes (general notation PgC*n*, **2**; Figure 1).[2–6] We have also shown that the latter form noncovalent nanotubes in the solid state under particular solvent conditions.[7] For CMRC, six calixarene building blocks assemble with eight structural water molecules into a near-spheroidal hexamer, which is stabilized by concerted hydrogen bonding.[2] Pyrogallol[4]arenes contain additional "upper-rim" hydroxy groups compared to CMRC which results in a larger number of hydrogen-bonding interactions per hexamer formed, preclusion of structural water molecules from the hydrogen-bonded capsule seam, and enhanced stability of the nanocapsule.[4–6] Alternative covalent approaches have been used to form pentameric "superbowls"[8a] or hexameric calixarene-based assemblies of relatively comparable size to those described above;[8b,c] however, inclusion of non-solvent guests is yet to be reported for such arrangements. Furthermore, metal-coordination approaches have also been used to form completely or partially sealed pyrogallol[4]arene-based hexamers.[9]

Some of our recent studies focused on the use of a fluorescent probe molecule (pyrene butyric acid, PBA) to report on the order of the inner phase of a PgC_6 hexamer (hexamer framework shown as $(\mathbf{2a})_6$ in Figure 1).[6e] This process involved the addition of a quenching agent (dimethylaniline, DMA) to a solution of the PBA-containing hexamers, the overall structures of which were found to be stable in the solution phase. Given this result, we sought to encapsulate a fluorescent probe molecule with a built-in

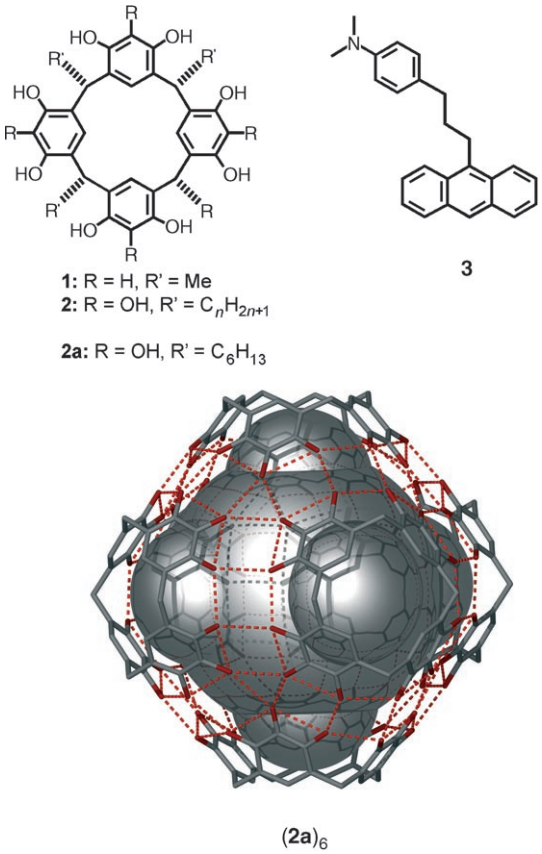

Figure 1. Structures of CMRC (**1**), PgC*n* (**2**), PgC_6 (**2a**), and ADMA (**3**), and a diagram of the PgC_6 hexamer framework $(\mathbf{2a})_6$ showing the possible space for molecular encapsulation (framework shown in stick representation: C gray, O red; internal volume shown in gray space-filling representation).

quencher to further examine the capsule microenvironment in terms of conformational restriction and probe movement. For this purpose, we selected 4-[3-(9-anthryl)propyl]-*N*,*N*-dimethylaniline (ADMA, **3**) as a probe for inclusion in the $(\mathbf{2a})_6$ nanocapsule. Following excitation of the anthryl moiety, the ADMA fluorophore can undergo charge transfer by accepting an electron from the DMA fragment. Furthermore, exciplex formation may be observed as the DMA portion folds to form a sandwich-like arrangement with the anthryl moiety.[10]

By using the same procedures employed for the inclusion of PBA, ADMA was found to crystallize either *exo* (occasionally) or *endo* (frequently) with respect to the $(\mathbf{2a})_6$ framework (see Supporting Information).[6e] For the *exo*-capsule ADMA array, small, colorless, cubic-shaped crystals occasionally grew during the slow evaporation step. Structural analysis showed the probe to be *exo* to the nanocapsule and to form an unexpected supramolecular array by intercalating between hexamers, forming channels in the solid state. For the *endo*-capsule ADMA array, the unit cell parameters of the crystals were identical to those of the pure acetonitrile (MeCN) solvate.[11] On examining the crystals under a UV lamp (365 nm), the observation of strong fluorescence confirmed the presence of the fluorophore within the nanocapsules. Herein, we report the single-crystal X-ray structure

[*] Dr. S. J. Dalgarno, D. B. Bassil, Dr. S. A. Tucker, Prof. J. L. Atwood
Department of Chemistry
University of Missouri-Columbia
601 South College Avenue, Columbia, MO 65211 (USA)
Fax: (+1) 573-882-2754
E-mail: tuckers@missouri.edu
atwoodj@missouri.edu

[**] We thank the NSF for financial support.
Supporting information for this article is available on the WWW under http://www.angewandte.org or from the author.

of the *exo*-capsule ADMA array, unit cell dimensions of crystals of the *endo*-capsule ADMA array, and solution-phase studies for both structural arrangements that show markedly different probe behavior.

Single-crystal X-ray diffraction studies of crystals of the *exo*-capsule ADMA array revealed them to be weakly diffracting.[12a] The crystals were in a triclinic system, and solution of the structure showed the asymmetric unit to contain half of a hexameric nanocapsule, a total of 1.5 molecules of ADMA disordered over four positions (stoichiometry confirmed by ^{1}H NMR spectroscopy; see Supporting Information), and a number of badly disordered acetonitrile molecules. The most noticeable feature of the asymmetric unit is that the probe is *exo* to the large internal cavity of the PgC_6 nanocapsule. Although there is significant disorder present within the structure, symmetry expansion of the asymmetric unit reveals a number of very interesting features in the extended array when compared with the simple PgC_6 MeCN solvate nanocapsule.[11] The structure is described in three parts: nanocapsule packing differences, interactions associated with full-occupancy ADMA, and the environment surrounding the badly disordered half-occupancy ADMA.

Examination of the packing of neighboring nanocapsules in the MeCN solvate structure revealed that the hexamers pack in a near-cubic-close-packed arrangement (Figure 2a).[11] The walls of neighboring nanocapsules (aligned along the *a* axis, Figure 2b) were found to interact through π stacking between aryl rings, thereby resulting in a short intercapsule distance of 19.573 Å (see Supporting Information for a full depiction of the intercapsule distances for both structures). The structure of the *exo*-capsule ADMA array revealed that the packing of adjacent hexamers is altered, as shown by the capsule spacings in Figure 2c (and the intercapsule distances listed in the Supporting Information, the shortest of which is 22.026 Å). When comparing the nanocapsules aligned along the *a* axes (Figure 2b and d), these appear to be slipped relative to the MeCN solvate and instead of π stacking, there is a crystallographically unique CH···π interaction from a neighboring PgC_6 hexyl chain to an aromatic ring with a CH···aryl centroid distance of 3.386 Å.

Upon examining the environment of the ADMA that is at full-occupancy over two closely disordered positions, numerous CH···π, CH···O, and π-stacking interactions are observed between the probe and neighboring molecules (observable to some extent in Figure 3). Perhaps the most influential of these interactions occurs between the faces of neighboring nanocapsules: two ADMA molecules (related by an inversion center) dimerize through N···aryl interactions from the nitro-

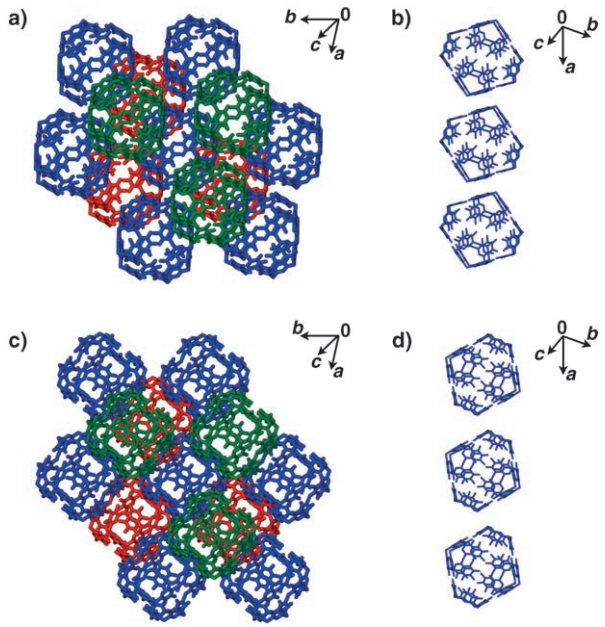

Figure 2. Comparison of the solid-state packing of PgC_6 hexamers in the MeCN solvate (a and b), and in the *exo*-capsule ADMA array (c and d). For the MeCN solvate, the hexameric nanocapsules form a near-cubic-close-packed arrangement (a) with π-stacking interactions between neighboring faces (b).[11] In the structure of the *exo*-capsule ADMA array, the nanocapsules pack with some larger intercapsule spacings (between centroids), as can be seen, for example, by the separation of blue nanocapsules along the *ab* diagonal (all separations are shown in the Supporting Information). For comparison with the MeCN solvate, the closest face-to-face interactions (b and d) show the hexamers in the *exo*-capsule ADMA array to be "slipped" in their alignment along the *a* axis.[11]

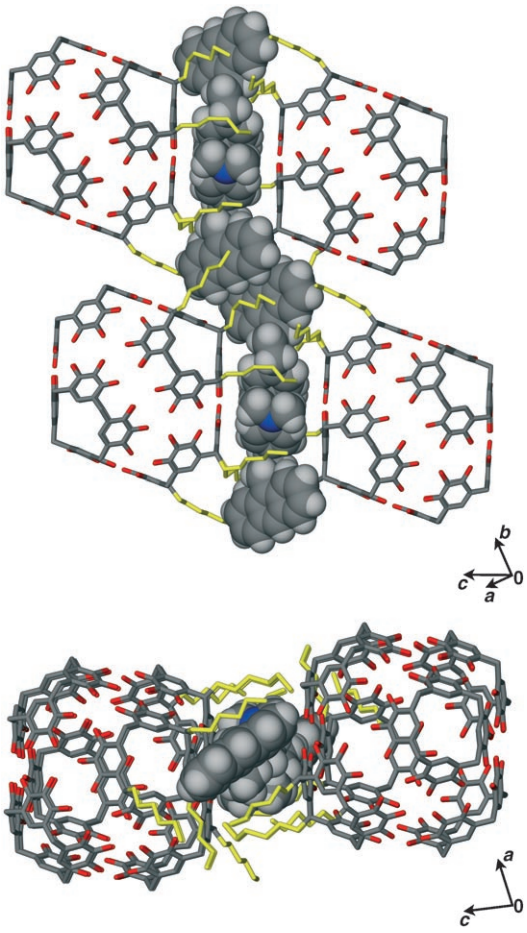

Figure 3. Two views of the ADMA channels (space-filling representation: C gray, N blue) formed by fluorophore intercalation between walls of neighboring nanocapsules (stick representation: C gray, O red). The PgC_6 hexyl chains proximate to the ADMA channels are shown in yellow, whilst all others are removed for clarity.

gen atom of one DMA fragment to the aromatic ring of the symmetry-related DMA moiety (N···aryl centroid distance of 2.755 Å). Also, aryl hydrogen atoms of the DMA fragments form CH···π interactions to neighboring aryl rings of nanocapsule walls, with CH···aryl centroid distances of 2.818 and 3.361 Å. The proximate PgC_6 hexyl chains wrap around the probe molecules and interact through numerous CH···π interactions. The result of these concerted interactions is the formation of an ADMA channel within the extended structure (Figure 3).

The structure is badly disordered in the region containing the half-occupancy ADMA molecule, which is also disordered over two positions. This molecule occupies discrete interstitial sites between nanocapsules (completely surrounded by PgC_6 molecules/hexyl chains) that are also partially occupied by disordered *C*-hexyl chains. Given the extent of the disorder, it was not possible to precisely identify intermolecular interactions for discussion here.

To some extent, the solution-state results are consistent with the solid-state structure.[13] In THF, free ADMA shows clear exciplex emission at 550 nm as a result of charge transfer (CT, Figure 4a).[14] Crystals of the *exo*-capsule ADMA array were dissolved in dry THF and shaken for approximately 5 minutes prior to study of the fluorescence emission. The fluorescence emission intensity of the anthracene moiety of ADMA in the dissolved crystal solution increased by approximately 40% relative to free ADMA and is attributed to the intercalation of the probe between the nanocapsule assemblies. The exciplex emission intensity is reduced, which

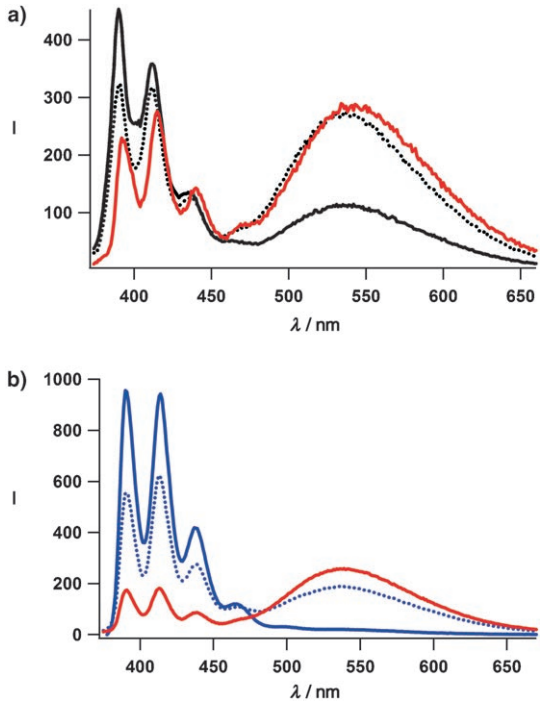

Figure 4. Spectral profiles (relative fluorescence intensities (I)): a) Free ADMA in THF (red), as well as the *exo*-capsule ADMA array in THF before (solid black line) and after sonication (dotted black line). b) Free ADMA in THF (red), as well as the *endo*-capsule ADMA array in THF at day zero (solid blue line) and after 14 days (dotted blue line).

is presumably due to enforced elongation of the ADMA molecules that are sandwiched in the channels between adjacent hexamers (black line, Figure 4a). To determine if this was the case, the solution was sonicated for 2 minutes and reexamined. Post sonication, the proposed structure/aggregate in solution appears to break apart, thereby releasing ADMA and allowing folding to occur; the emission spectrum resembles that of free ADMA in THF (Figure 4a). The spectral profile measured 12 h after sonication did not change, that is, the emission from ADMA in the sample remains similar to that of free ADMA in THF. This result indicates that at this concentration (10^{-6} M), ADMA does not reassociate with the nanocapsules to a significant extent, which would be identifiable by changes in the fluorescence emission spectrum.

For the *endo*-capsule ADMA array, unit cell dimensions of the single crystals closely matched those found for the PBA-containing nanocapsules and the MeCN solvate of $(\mathbf{2a})_6$.[6e,11,12b] Structural analysis showed the PgC_6 nanocapsule as expected, although the interior volume showed a complete lack of order. ^{1}H NMR spectroscopy revealed that the ADMA occupancy in the capsules was approximately 50%, assuming that each nanocapsule accommodates only one guest (see Supporting Information).[15]

Solution studies of crystals of the *endo*-capsule ADMA array dissolved in THF are consistent with the solid-state structure observed—they show that **3** *is* encapsulated in the MeCN-containing nanocapsule and does not reside exterior to the capsule in THF.[13] The fluorescence emission spectrum of the *endo*-capsule ADMA array (Figure 4b) shows little, if any, CT emission, which is consistent with the fact that the ADMA CT complex is not emissive in pure MeCN. Given that the crystals were grown from MeCN, **3** must be either encapsulated in a MeCN microenvironment or significantly constrained, as the presence of THF would cause prominent exciplex emission. Compared to free ADMA, the fluorescence emission intensity of the anthracene moiety of the *endo*-capsule ADMA array is dramatically increased (Figure 4b). This enhancement is attributed to the structural constraints imposed by the nanocapsule and to the protective nature of the host structure that most likely minimizes the possibility of non-radiative, excited-state deactivation, such as collisional quenching by solvent molecules.

In our previous studies concerning the encapsulation of PBA within $(\mathbf{2a})_6$, guest-to-wall binding was observed in both the solution and solid states, and was attributed to π-stacking and CH···π interactions between PBA and aryl rings of PgC_6 molecules.[6e] There is no spectral evidence to suggest that this type of interaction occurs with **3**. Moreover, the amount of PBA that leached from the capsules over 4 weeks, as measured by exciplex formation with DMA, was about 10%. The structural integrity of the the *endo*-capsule ADMA assembly is uncertain at this point. After 14 days, CT emission appears in the spectral profile, indicating either that around 40% of the encapsulated ADMA leaches from the capsules (Figure 4b) or that THF enters the capsule thereby facilitating CT emission.

To conclude, we have shown that relatively small molecules can dramatically change the extended packing of large

robust supramolecular entities through a series of noncovalent interactions. Intercalated *exo*-capsule ADMA offers the opportunity to study the arrangement in the solution phase through fluorescence spectroscopy, and future studies will focus on both steady-state and dynamic fluorescence techniques with the possibility of elucidating nanocapsule dispersion times in the solution phase. Studies on encapsulated ADMA continue with a view to examining the stability of the assembly, as well as the fluorescence lifetime and conformational behavior of the guest.

Received: May 17, 2006
Published online: October 2, 2006

Keywords: calixarenes · charge transfer · fluorescence · structure elucidation · supramolecular chemistry

[1] J.-M. Lehn, *Supramolecular Chemistry: Concepts and Perspectives*, VCH, Weinheim, **1995**; J. W. Steed, J. L. Atwood, *Supramolecular Chemistry: A Concise Introduction*, Wiley, Chichester, **2000**.

[2] L. R. MacGillivray, J. L. Atwood, *Nature* **1997**, *389*, 469 – 472.

[3] A. Shivanyuk, J. Rebek, Jr., *Chem. Commun.* **2001**, *22*, 2374 – 2375; A. Shivanyuk, J. Rebek, Jr., *J. Am. Chem. Soc.* **2003**, *125*, 3432 – 3433; M. Yamanaka, A. Shivanyuk, J. Rebek, Jr., *J. Am. Chem. Soc.* **2004**, *126*, 2939 – 2943; J. Rebek, Jr., *Angew. Chem.* **2005**, *117*, 2104 – 2115; *Angew. Chem. Int. Ed.* **2005**, *44*, 2068 – 2078; L. C. Palmer, J. Rebek, Jr., *Org. Lett.* **2005**, *7*, 787 – 789.

[4] T. Gerkensmeier, W. Iwanek, C. Agena, R. Frölich, S. Kotila, C. Näther, J. Mattay, *Eur. J. Org. Chem.* **1999**, 2257 – 2262.

[5] L. Avram, Y. Cohen, *Org. Lett.* **2003**, *5*, 3329 – 3332; L. Avram, Y. Cohen, *J. Am. Chem. Soc.* **2003**, *125*, 16180 – 16181; L. Avram, Y. Cohen, *J. Am. Chem. Soc.* **2005**, *127*, 5714 – 5719; Y. Cohen, L. Avram, L. Frish, *Angew. Chem.* **2005**, *117*, 524 – 560; *Angew. Chem. Int. Ed.* **2005**, *44*, 520 – 554.

[6] a) J. L. Atwood, L. J. Barbour, A. Jerga, *Chem. Commun.* **2001**, *22*, 2376 – 2377; b) J. L. Atwood, L. J. Barbour, A. Jerga, *J. Supramol. Chem.* **2002**, *1*, 131 – 134; c) J. L. Atwood, L. J. Barbour, A. Jerga, *Proc. Natl. Acad. Sci. USA* **2002**, *99*, 4837 – 4841; d) G. W. V. Cave, J. Antesberger, L. J. Barbour, R. M. McKinlay, J. L. Atwood, *Angew. Chem.* **2004**, *116*, 5375 – 5378; *Angew. Chem. Int. Ed.* **2004**, *43*, 5263 – 5266; e) S. J. Dalgarno, S. A. Tucker, D. B. Bassil, J. L. Atwood, *Science* **2005**, *309*, 2037 – 2039.

[7] S. J. Dalgarno, G. W. V. Cave, J. L. Atwood, *Angew. Chem.* **2006**, *118*, 584 – 588; *Angew. Chem. Int. Ed.* **2006**, *45*, 570 – 574.

[8] a) E. S. Barrett, J. L. Irwin, A. J. Edwards, M. S. Sherburn, *J. Am. Chem. Soc.* **2004**, *126*, 16747 – 16749; b) D. A. Makeiff, J. C. Sherman, *J. Am. Chem. Soc.* **2005**, *127*, 12363 – 12367; c) X. Liu, Y. Liu, G. Li, R. Warmuth, *Angew. Chem.* **2006**, *118*, 915 – 918; *Angew. Chem. Int. Ed.* **2006**, *45*, 901 – 904.

[9] R. M. McKinlay, G. W. V. Cave, J. L. Atwood, *Proc. Natl. Acad. Sci. USA* **2005**, *102*, 5944 – 5948; R. M. McKinlay, P. K. Thallapally, G. W. V. Cave, J. L. Atwood, *Angew. Chem.* **2005**, *117*, 5879 – 5882; *Angew. Chem. Int. Ed.* **2005**, *44*, 5733 – 5736.

[10] T. J. Chuang, R. J. Cox, K. B. Eisenthal, *J. Am. Chem. Soc.* **1974**, *96*, 6828 – 6831.

[11] S. J. Dalgarno, R. M. McKinlay, J. Antesberger, J. L. Atwood, unpublished results.

[12] a) Crystal data for the *exo*-capsule ADMA array: $C_{209}H_{276.75}N_{9.25}O_{36}$, $M_r = 3494.65$, triclinic, $a = 22.026(3)$, $b = 22.631(3)$, $c = 24.430(3)$ Å, $\alpha = 73.184(3)$, $\beta = 65.777(3)$, $\gamma = 77.975(3)°$, $U = 10575(2)$ Å^3, $\mu = 1.098$ mm^{-1}, $T = 173(2)$ K, space group $P\bar{1}$, $Z = 2$, $Mo_{K\alpha}$ radiation ($\lambda = 0.71073$ Å), GOF = 1.066, agreement index $R_1 = 0.1657$, 59608 reflections measured, 44761 unique ($R_{int} = 0.0933$) which were used in all calculations. The final $\omega R(F^2)$ value was 0.4536 (all data). The crystals were weakly diffracting and the structure has a number of badly disordered regions. CCDC 603842 contains the supplementary crystallographic data for this paper. These data can be obtained free of charge from The Cambridge Crystallographic Data Centre via www.ccdc.cam.ac.uk/data_request/cif. b) Unit cell dimensions for the *endo*-capsule ADMA array (crystal structure): triclinic, $a = 19.5574(41)$, $b = 22.6032(47)$, $c = 23.4174(49)$ Å, $\alpha = 69.7844(34)$, $\beta = 70.0905(41)$, $\gamma = 71.9823(37)°$, $U = 8915(5)$ Å^3. This data was not submitted to the CCDC as no structural information relating to the interior volume of the nanocapsule could be reported as a result of the disorder and guest occupancy ($\approx 50\%$). These dimensions are consistent with those of the acetonitrile solvate for $(\mathbf{2a})_6$ and $(\mathbf{2a})_6 \cdot 1.5$ PBA.[6c,11]

[13] All measurements were performed at optically dilute concentrations (10^{-6} M) of ADMA (free, *exo*, or *endo*) in THF at room temperature. Fluorescence emission spectra were measured on a Varian Cary Eclipse Fluorometer with the following parameters: 15-W xenon arc lamp (pulsed at 80 Hz), excitation and emission step size of 2 nm, and a bandpass of 5 nm.

[14] M. Khajepour, J. F. Kauffman, *J. Phys. Chem. A* **2000**, *104*, 7151 – 7159.

[15] The occupancy is relatively low compared to that found for encapsulated PBA (1.5 molecules per hexamer), and given the fact that ADMA could be oriented over three equivalent axes within the crystal structure it is the likely reason for the irresolvable nature of the capsule interior.

